NASA TECHNICAL MEMORANDUM

NASA TM X-2304

NASA TM X-2304

FEASIBILITY STUDY OF JET-FUEL-COOLED PLUG NOZZLE FOR AFTERBURNING TURBOJET

by Francis S. Stepka and Rene E. Chambellan

Lewis Research Center

Cleveland, Ohio 44135

NATIONAL AERONAUTICS AND SPACE ADMINISTRATION • WASHINGTON, D. C. • JUNE 1971

1. Report No.	2. Government Accession No.	3. Recipient's Catalog No.
NASA TM X-2304		

4. Title and Subtitle	5. Report Date
FEASIBILITY STUDY OF JET-FUEL-COOLED PLUG NOZZLE FOR AFTERBURNING TURBOJET	June 1971
	6. Performing Organization Code
7. Author(s)	8. Performing Organization Report No.
Francis S. Stepka and Rene E. Chambellan	E-6022
	10. Work Unit No.
9. Performing Organization Name and Address	720-03
Lewis Research Center National Aeronautics and Space Administration Cleveland, Ohio 44135	11. Contract or Grant No.
	13. Type of Report and Period Covered
12. Sponsoring Agency Name and Address	Technical Memorandum
National Aeronautics and Space Administration Washington, D. C. 20546	14. Sponsoring Agency Code

15. Supplementary Notes

16. Abstract

A conceptual design was made of a fuel-cooled plug nozzle. Factors affecting cooling, fuel coking, construction and strength were considered. Results indicate that the total available engine fuel flow was sufficient to restrict the maximum temperature of the metal contacting fuel to 817 K (1010° F) or less. Even at this maximum temperature, coking of cooling tubes is not expected to be significant for at least 100 hours of engine operation, based on experimental results of others with low-oxygen-content jet fuel flowing in heated tubes.

17. Key Words (Suggested by Author(s))	18. Distribution Statement
Exhaust nozzle Plug nozzle Heat transfer Fuel-cooling	Unclassified - unlimited

19. Security Classif. (of this report)	20. Security Classif. (of this page)	21. No. of Pages	22. Price*
Unclassified	Unclassified	36	$3.00

*For sale by the National Technical Information Service, Springfield, Virginia 22151

FEASIBILITY STUDY OF JET-FUEL-COOLED PLUG NOZZLE FOR AFTERBURNING TURBOJET

by Francis S. Stepka and Rene E. Chambellan

Lewis Research Center

SUMMARY

A conceptual design and feasibility study was made of an exhaust-plug nozzle cooled by jet engine fuel. In the analysis of the design, the various factors that would affect cooling, coking, construction, and structural characteristics were considered. Factors particularly evaluated were coolant passage spacing, tube wall thickness, and braze fillet size. The aerodynamic surface of the plug consisted of a 0.813-millimeter (0.032-in.) thick sheet metal shell covered internally with equally spaced 3.15-millimeter (1/8-in.) inside-diameter tube coolant passages wound in a modified helical pattern. Cooling tube wall thicknesses of 0.076 and 0.254 millimeter (0.003 and 0.010 in.) were considered.

In the analysis, the following operating conditions for the nozzle were considered: engine at sea level take-off conditions with and without afterburning and at conditions of flight at an altitude of 13 716 meters (45 000 ft) at Mach 1.2 with afterburning. The afterburner gas temperature was as high as 2020 K (3177° F).

Results of the analyses indicated that the maximum local temperature of the metal in contact with the fuel can be kept to 817 K (1010° F). Tube metal temperatures at other locations are considerably less. Coking at even the maximum temperature is not expected to be significant for at least 100 hours of engine operation with low-oxygen-content jet fuel. Furthermore, any coke accumulated in the coolant tubes could be burned off by passing air, at temperatures around 921 K (1200° F), through the tubes while the engine is not operating, or by passing air through the tubes when the afterburner is off and the turbine exit temperature is about 983 K (1310° F).

A weight analysis showed that the dry weight of the plug and supporting structure assembly when 0.076-millimeter (0.003-in.) thick cooling tubes were used was 27 kilograms (60 lbm) and the wet weight of the assembly was 35 kilograms (77 lbm). The engine for which this plug was designed is an afterburning turbojet with a sea-level take-off thrust of 18 400 newtons (4100 lbf).

INTRODUCTION

This report describes and presents the results of an analytical study to determine the feasibility of a lightweight exhaust nozzle plug cooled with jet engine fuel. A description of a preliminary design is presented for a fuel-cooled plug nozzle intended to be compatible with the requirements of an afterburning turbojet engine for an advanced supersonic aircraft.

An important advantage in the use of a plug nozzle is its ability to maintain relatively high aerodynamic performance over a wide range of nozzle pressure ratios when compared with the conventional movable iris-type nozzle (ref. 1). Other advantages are noise reduction and reduction of infrared radiation from the rear end of the engine because of the relatively low wall temperatures of the plug. Disadvantages that have inhibited its use are associated with cooling and structural support.

One way to cool a nozzle plug is by convective (ref. 2) or film cooling (ref. 3) modes of heat transfer, using tertiary air and bleed air from the engine compressor. This approach, however, can penalize the engine cycle and nozzle efficiency, depending on the amount and the way that cooling air is used. Another cooling method is to use engine fuel with its large heat-absorbing capacity. With this method, the heat absorbed by the fuel in cooling the plug is returned to the cycle. However, there are several problems associated with fuel cooling. Those of primary importance are coking, clogging, and possible burn-out of the cooling tubes. Other potential problems are (1) high thermal stresses in structural components due to the large temperature differences that exist between the coolant tubes and the plug shell, (2) possible carburization of the coolant passage material and consequent reduction in ductility for metal temperatures exceeding about 922 K (1200° F) (ref. 4), and (3) possible coolant flow instability accompanied by large pressure fluctuations (apparently caused by large temperature and density gradients in the fuel at the heated surface), which can result in potential damage to the coolant tubes (ref. 5).

The preliminary design of a fuel-cooled plug nozzle, reported herein, was made compatible with maximum allowable fuel and metal temperatures. The basis for the temperature limits was obtained from both published (refs. 6 and 7) and unpublished experimental investigations (by Shell Development Company under NASA Contract NAS3-12432) of coking in heated tubes containing flowing fuel.

The contour and size of the plug nozzle used in this design study was the same as the plug studied in reference 8. The reference describes the nozzle in detail, and presents its internal aerodynamic performance. The plug was designed to fit the exhaust section of a small afterburning turbojet engine with a sea level static thrust of about 18 400 newtons (4100 lbf).

The analysis used in this report included factors that would affect plug cooling, coking, structural details, and construction. Particular factors were coolant passage spacing, tube wall thickness, and braze fillet size. The exhaust gas temperatures used in the analyses were as high as 2020 K (3177° F) and 983 K (1310° F) for afterburning and nonafterburning conditions, respectively. The temperatures of the fuel supplied to the plug were assumed to be 311 K (100° F) with afterburning and either 311 or 367 K (100° or 200° F) with no afterburning. The fuel was assumed to be jet A, and its supply pressure was 4.13×10^6 N/m^2 (600 psia). The analysis was performed using U.S. Customary Units.

CONFIGURATION OVERALL DESCRIPTION

The nozzle plug, illustrated schematically in figure 1, is a streamlined shell of revolution, truncated at the rear end, and situated at the rear end of the engine afterburner section. The plug studied here is supported by a cantilevered tube which is anchored to the hub of a cruciform beam structure, located just aft of the turbine. The dimensions of the plug-nozzle are shown in figure 2. A more detailed cross-section view for the fuel cooled plug is shown in figure 3.

The support tube provides the restraints necessary to keep the plug in position. In addition to supporting the plug, the support tube provides protection and support for the coolant tubes. Concentric to the support tube are two internal tubes. The annular space between the central or smallest tube and the intermediate tube provides the passage for supply of the coolant fuel to the distribution manifold at the rear of the plug. The annular space between the intermediate tube and the support tube provides a duct for the coolant return tubes. Finally, the space inside the smallest concentric tube provides a duct for instrumentation leads.

The forward end of the plug is subjected to a maximum gas pressure of 24.4 N/cm^2 (35.53 psia). The shell thickness of the plug frontal cone is 0.813 millimeter (0.032 in.) and requires support to prevent buckling. Figure 3 shows an internal stiffening ring with T cross-section which is located about 17.8 centimeters (7 in.) forward of the plug nozzle throat. A support diaphragm has been provided at the throat section to keep the plug shell centered with respect to the intermediate tube and, in addition, provide stiffening for the shell. The plug shell behind the throat is also 0.813 millimeter (0.032 in.) thick but requires no internal supports to resist buckling since the pressures are very low. The internal volume of the plug is vented overboard to ambient pressure conditions.

Cooling of the plug assembly is accomplished by a single pass, parallel flow of the coolant which flows from a location at the forward end of the afterburner section, through the plug, and back to the front end of the afterburner section. The coolant is

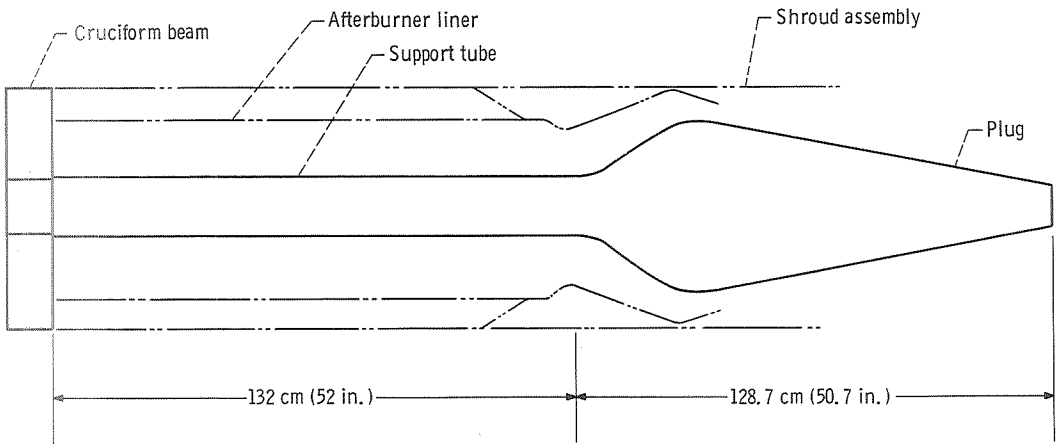

Figure 1. - Plug-nozzle assembled in afterburner.

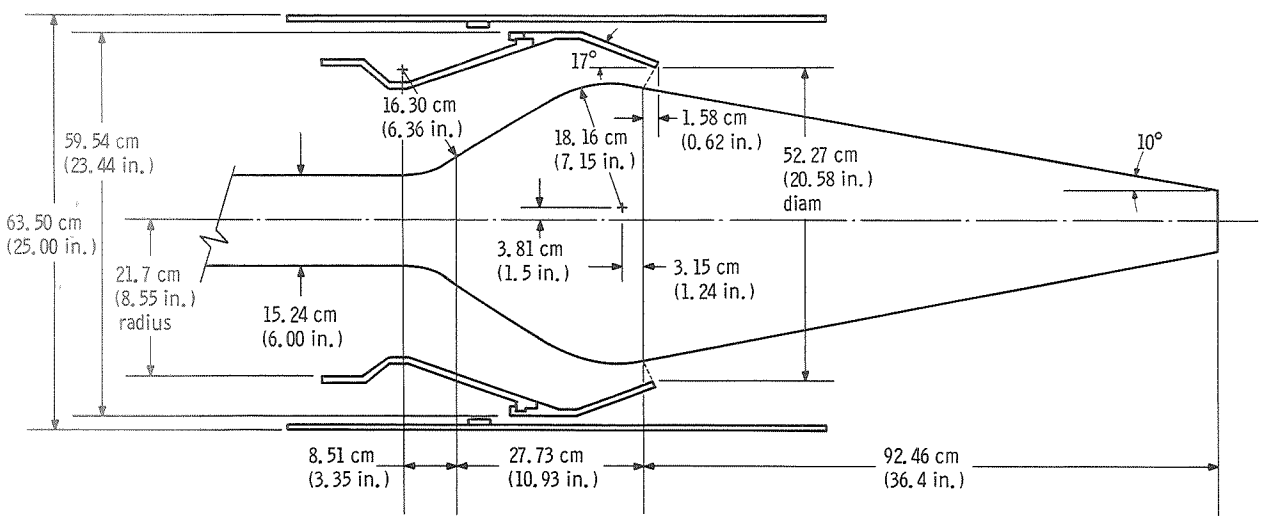

Figure 2. - Plug-nozzle dimensions.

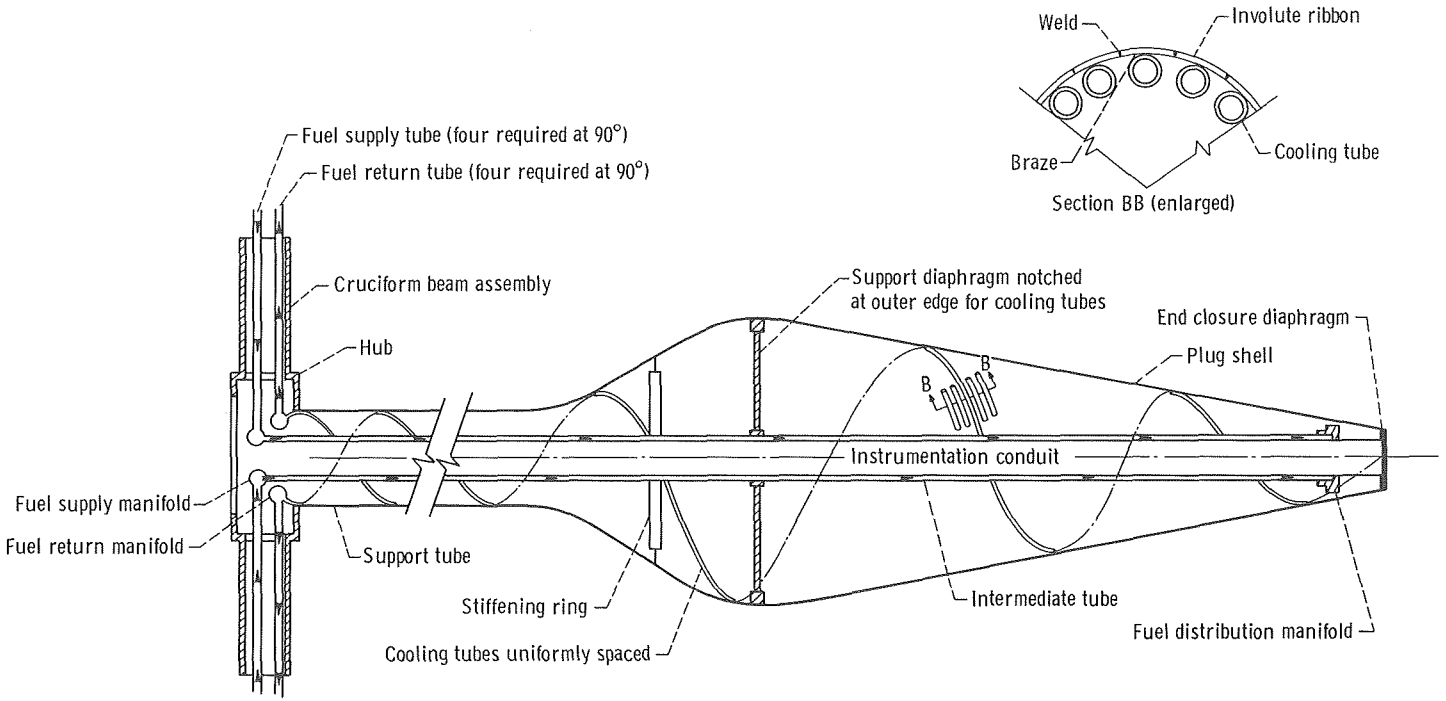

Figure 3. - Fuel-cooled nozzle plug assembly.

furnished to the plug assembly through a toroidal supply manifold located in the cruciform beam hub (fig. 3). The coolant flows from the supply manifold through the annular space between the central and intermediate tubes, within the support tube. This annular space is connected to the coolant distribution manifold at the rear of the plug. The plug shell cooling tubes are connected to the rear distribution manifold, follow the inside surface contour of the shell, and return through the annular space between the support and intermediate tubes. The shell cooling tubes are joined to the inner surface of the shell and support tube following a modified helical path. Constant tube spacing is maintained everywhere on the shell and support tube surface. The tubes are then connected into the return toroidal manifold. From this manifold the heated fuel is conducted to a valve which connects to the afterburners or the engine combustors or both.

CONDITIONS AND CRITERIA FOR DESIGN

Gas and Fuel Conditions

Three conditions of exhaust gas conditions were studied: nonafterburning and maximum afterburning (AB) at sea level and maximum afterburning at an altitude of 13 716 meters (45 000 ft) at a Mach number of 1.2. A summary of pertinent parameters at these conditions (obtained from ref. 9) appears in the following table:

	Sea level maximum afterburning	Sea level nonafterburning	Maximum afterburning at Mach 1.2 at 13 716 m (45 000 ft)
Total gas temperature, K (^{o}F)	2036 (3177)	985 (1310)	2023 (3154)
Total gas pressure, N/cm^2 (psia)	24.5 (35.53)	24.5 (35.53)	8.5 (12.38)
Nozzle pressure ratio	2.13	2.29	5.09
Engine air flow rate, kg/sec (lbm/sec)	19.96 (44)	19.96 (44)	7.08 (15.6)
Afterburner fuel flow rate, kg/hr (lbm/hr)	2812 (6200)	----------	1110 (2448)
Primary burner fuel flow rate, kg/hr (lbm/hr)	1309 (2886)	1277 (2815)	478 (1053)
Assumed fuel supply pressure, N/cm^2 (psia)	413 (600)	413 (600)	413 (600)
Assumed fuel supply temperature to plug nozzle, K (^{o}F)	310 (100)	310 and 367 (100 and 200)	310 (100)

When afterburning, the total gas temperature along the support tube (fig. 1) was assumed to rise linearly with distance as combustion proceeds. The temperature starts at a turbine exit temperature of 985 K (1310° F) and is assumed to rise to the final gas total temperature (shown in above table) at the junction of the support tube and plug.

The fuel pressure shown in the table was selected to be sufficiently high so as to remain above the fuel critical pressure within the plug assembly. This pressure avoids possible problems associated with two phase flow, such as increased coking (ref. 6) and flow instabilities. The pressure assumed is over twice the fuel critical pressure. The fuel critical pressure and temperature are 182 N/cm^2 (265 psia) and 653 K (716° F), respectively.

When afterburning, the plug assembly is assumed to be cooled by both primary combustor and afterburner fuel flows. In order to provide for instant afterburner light-off and to avoid large transient thermal stresses in the structure flow instabilities and coking problems, the primary combustor fuel is assumed to be flowing through the cooling tubes even when the afterburner is not lit. For this condition heat-transfer calculations were made for the two fuel supply temperatures shown in the previous table. The higher temperature is considered because the primary fuel is often heated in engine lube-to-fuel and hydraulic fluid-to-fuel heat exchangers prior to being burned.

Criteria to Limit Coking and Carburization

The diameter of the shell cooling tubes was chosen to be small enough to provide a sufficiently high fuel-side heat-transfer coefficient, but large enough to provide a low probability of becoming choked with solid deposits from the fuel. A tube inside diameter of 3.15 millimeters (about 1/8 in.) was selected since satisfactory results with about this diameter were obtained in tests reported in references 6 and 7. In the tests of reference 6, heated tubes of 3.18 millimeters (1/8 in.) inside diameter with jet A fuel flowing for periods of 20 hours showed only slight coking with wall temperatures up to 755 K (900° F) and bulk fuel temperatures of 644 K (700° F). Tests results reported in reference 7 showed that more costly, highly refined paraffinic fuel, F-71, can be used at bulk temperatures in excess of 811 K (1000° F) and even higher wall temperatures without excessive coking for several hours.

Recent and more encouraging results with low-oxygen-content (about 0.5 ppm) jet A fuel flowing through heated tubes (as yet unpublished) were obtained by Shell Development Company under contract to NASA (Contract NAS3-12432). As part of the study, flowing fuel was subjected to a heat flux of 1.635×10^6 J per second per square meter (1 Btu/(sec)$(in.^2)$) for 100 hours during which the average tube wall temperature was about 978 K (1300° F) and the outlet fuel temperature was 811 K (1000° F). Although

pressure fluctuations (similar to those observed in ref. 5) were obtained after 50 hours and persisted until the 75th hour, the tubes completed 100 hours of operations. Examination of the tubes indicated that the coke deposit was less than 0.025 millimeter (0.001 in.) thick.

Based on these results and those in references 6 and 7, operation of a fuel-cooled plug nozzle for at least 100 hours without significant coke deposit can be expected if the maximum fuel tube inside wall temperature and the fuel exit temperature were limited to 922 and 755 K (1200° and 900° F). These temperatures were considered to be the allowable design limits.

The number of cooling tubes wound around the plug was selected to provide for a two or three tube diameter lateral spacing (fig. 3) and to provide turbulent flow (Reynolds number above 2300) at the tube entrance. Thus, there were 50 tubes for the two-diameter and 34 tubes for the three-diameter lateral spacings between tubes. The calculated fuel flow Reynolds numbers ranged from 2.5×10^3 to 2.0×10^5. The fuel velocities in the tubes ranged from 1.1 to 7.3 meters per second (4 to 24 ft/sec).

Criteria for Structural Design

Design loadings. - Typical design loadings for the plug nozzle considered were assumed to be

(1) Afterburner chamber pressure, 34.5 N/cm^2 (50 psia)

(2) Steady state fuel pressure, 413 N/cm^2 (600 psia)

(3) Peak fuel pressure, 621 N/cm^2 (900 psia)

(4) Plug internal pressure, ambient atmospheric

(5) Longitudinal acceleration, 10 g's

(6) Lateral acceleration, 4 g's

Mechanical properties of materials of construction. - The materials of construction for the plug shell and fuel tubes were assumed to be from the class of high-temperature, high-strength nickel-base superalloys such as René 41. The braze material was assumed to be a nickel manganese alloy such as Nicrobraz 230 (Wall Colmonoy Corp.). It was also assumed that the joints transmit working forces between adjacent parts in the assemblies without yielding.

DETAILS OF CONSTRUCTION

Construction and Assembly

Locating the cooling tubes on the inside surfaces of the plug and support tube presents difficult fabrication and assembly problems. A method has been developed, in

theory, for fabricating assemblies of plug shell elements, support tube elements, and cooling tubes in the form of flat, curved strips of a particular shape. The cooling tubes are brazed to that side of the strip that will be inside the plug, or support tube, when assembled. The plug shell and support tube is formed by winding a full set of strip-to-tube assemblies on a mandrel, and then welding the faying surfaces of adjacent strips. A cross-section normal to the plug shell and cooling tubes is shown in figure 3. This view shows the tube-to-shell braze and the strip-to-strip welds.

The mandrel used to support the strip to tube elements must be removable after assembly is complete. One method of construction would be to assemble all the plug internal members and then cast a mandrel of a low melting alloy or plaster of paris around these parts to form the shell surface of revolution. Suitable grooves would be formed in the cast mandrel to receive the coolant tubes and support the strip-to-tube assemblies during welding. After welding, the mandrel material would be removed by melting or dissolution, as appropriate. The next step in the assembly would be to join the plug and support tube assembly to the forward end manifolds and to the cruciform support beam. The coolant-tube assembly at the rear fuel supply manifold can be made by field brazing the tubes into prepared counterbores in the manifold.

Geometry of Cooling Tube and Shell Assemblies

The geometric definition of the curves required to produce the elemental strips that make up the plug shell is described in detail in reference 10. In principal, the shell surface is divided into continuous strips, from one end to the other, in a form that looks like a helix. The width of the strips can vary from strip to strip; however, in practice they would be assumed to be narrow and equal. The method for developing these strips is briefly described in the following.

The definition of the plane curved strip of the plug shell surface requires that the shell surface be developed onto a plane in a particular way. The plug shell surface is a double curved surface of revolution and therefore cannot be developed exactly on to a plane. An approximate method for accomplishing the development can be done in two steps. First, the surface of revolution is divided into a series of segments along the axis of symmetry, where these segments are approximated by developable surface elements such as cones and cylinders. The second step is to subdivide the developed approximating-surface-elements into ribbons of equal widths. The ribbon centerline for the entire plug is composed of a sequence of involute curves where each involute is associated with a particular plug segment. Each involute in the sequence is made tangent to the preceding involute, thus forming a composite involute curve. With the composite involute curve as the ribbon centerline, a continuous developed surface element of the

surface of revolution is formed. Accuracy of the shell contour produced by this method improves as the number of surface segments and involute strips increase.

The geometries of the cross-sections normal to the flow paths of the cooling tubes in the plug and in the support tube are shown in figure 4. The cooling tubes had an inside diameter of 3.15 millimeters (about 1/8 in.). A wall thickness of 0.076 millimeter (0.003 in.) was used for the majority of the analysis. The effect of increasing the wall thickness to 0.254 millimeter (0.010 in.) was determined. The tubes are shown as being bonded to the walls of the plug and support tube by two amounts of braze. The large amount of braze extending to 1.52 millimeters (0.06 in.) from the tube centerline is considered to be the full braze condition. The other one in which the braze extends only 0.51 millimeter (0.02 in.) from the tube centerline is considered to be the minimum braze condition. These two amounts of braze were selected as representing limits that could occur, depending on the manufacturing procedure rather than structural considerations. Variations in braze size along the tube lengths can be controlled by the selection of particular assembly methods. For example, brazing of the tubes to flat strips in a horizontal position provides greater control of braze fillet size than when part of the assembly permits the fillet to run in a vertical direction. These two limiting amounts of braze were considered in the heat transfer analysis to evaluate the effect of braze quan-

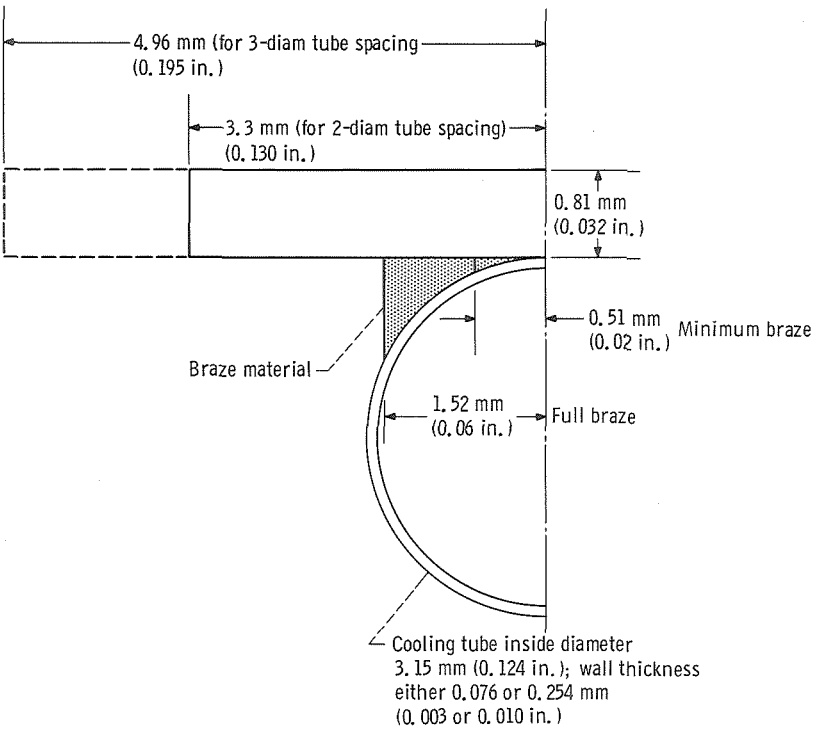

Figure 4. - Cross sections normal to fuel flow path through fuel-cooled plug nozzle.

tity on metal and fuel temperatures. Joining the tubes to the plug shell by brazing was selected for this study because it appears to be feasible for a prototype model. Other bonding methods may be devised which might simplify construction of a production type of nozzle.

Two spacings for cooling tubes were considered in this study. Figure 4 shows a two-tube and a three-tube diameter spacing. These spacings were considered in the heat-transfer analysis to assess the effect of tube spacing on metal temperatures.

METHOD OF ANALYSIS

Heat Transfer

The computer program of reference 11 was used to determine the temperature rise in the fuel as it flows through the cooling tube and the metal temperature distribution in the cross sections of the shell and cooling tubes of the plug and support tube.

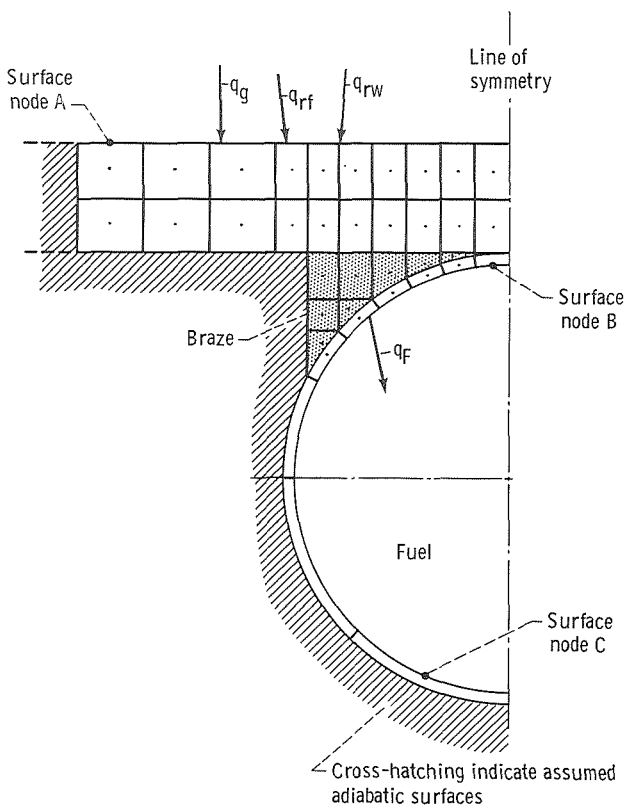

Figure 5. - Heat-transfer model.

The fuel flow paths in the plug and support tube were each divided into 10 equal lengths and a heat balance was made for each length. The heat-transfer model for the tube cross section including typical node breakdown is shown in figure 5. The heat flux into the plug or support tube shell would, in general, include convection from the hot gas q_g, radiation from the gas flame q_{rf}, and radiation interchange with tailpipe walls or other boundaries q_{rw}. In the analysis reported herein all the above heat fluxes were considered for the support tube. Radiation interchange with the plug, however, was not considered. The effect on fuel and tube wall temperatures was small, about 17 K (30° F).

The various heat inputs are conducted through the plug or support tube shell, through the braze material, through and around the cooling tube wall and finally into the fuel. In the heat transfer model it was assumed that the convective heat flow within the plug and support tube cavity, heat conduction along the length of the tube and shell, and the radiation interchange between the cooling tubes would be negligible. Therefore, as shown in figure 5, the inner surface of the plug or support tube wall, the outer boundaries of the braze material, and the outside surface of the cooling tube were assumed adiabatic. The cooling tubes and shell materials were assumed to have a thermal conductivity of 20.8 J/(sec)(m)(K) (12 Btu/(hr)(ft)($^{\circ}$F)), and that of the braze material 43.4 J/(sec)(m)(K) (25 Btu/(hr)(ft)($^{\circ}$F)).

The convective heat flux q_g into the plug or support tube shell for each incremental length of cooling tube was obtained from the equation,

$$q_g = h_g(T_{ge} - T_{wo}) \tag{1}$$

The terms are defined in the appendix. The gas-to-wall heat-transfer coefficient h_g was calculated by the method of reference 12. This method simultaneously solves the integral momentum and energy equations of the boundary layer in conjunction with a modified von Kármán momentum-heat analogy. The local Mach number, total gas temperature and pressure, plug geometry and local wall temperature, and the initial momentum boundary-layer thickness are required input data. An estimated wall outside surface temperature of 923 K (1200° F) and an initial momentum thickness of 0.025 millimeter (0.001 in.) were assumed. Repetition of the boundary-layer calculation using revised outside wall surface temperatures indicated that the effect of wall temperature on the coefficient was negligible; therefore, no further iterations were made. The initial momentum thickness assumed is considered conservative. Also, its effect decays after about 50.8 millimeters (2 in.) along the support tube. As a consequence, its effect on this study is insignificant.

The effective gas temperature T_{ge} was determined from the following equation from reference 12.

$$\frac{T_{ge}}{T_g} = \frac{1 + \Lambda\left(\frac{\gamma - 1}{2}\right)M_g^2}{1 + \frac{\gamma - 1}{2}M_g^2} \tag{2}$$

where $\Lambda = Pr_g^{1/3}$ and Pr_g assumed constant at 0.7. The value of T_{ge} was the average bulk effective gas temperature for each incremental length of the cooling tube. This assumption is conservative when afterburning in that a radial profile generally exists with the temperature near the wall being less than the average value in the passage (about 194 K (350° F) as obtained experimentally in ref. 2).

The radiation heat flux from the flame to the support tube q_{rf} was determined from the following equations (ref. 13);

$$q_{rf} = \frac{1}{2}\sigma(1 + \alpha_w)\epsilon_f T_f^{1.5}\left(T_f^{2.5} - T_{wo}^{2.5}\right) \tag{3}$$

and

$$\epsilon_f = 1 - \exp\left[-18.5\, p_g(\ell f)^{0.5}\, T_f^{-1.5}\right] \tag{4}$$

where for simplification the local fuel-air ratio f was assumed to be constant and the flame temperature T_f was assumed to be constant at the final afterburner gas temperature. Also the wall absorbtivity α_w was assumed to be 0.8.

The radiative heat flux interchange between the support tube and tailpipe wall q_{rw} was determined from the following equations (ref. 13):

$$q_{rw} = \frac{\sigma\epsilon_w^2}{2}\sum_{\text{all }\delta}\frac{r_t(r_t - r_s)^2\Gamma\left(T_{wt}^4 - T_{ws}^4\right)\delta}{r_s\left[(r_t - r_s)^2 + (X_s - X_t)^2\right]^{3/2}} \tag{5}$$

and

$$\Gamma = \frac{14.82}{p_p\sqrt{(X_s - X_t)^2 + (r_t - r_s)^2} + 14.82} \tag{6}$$

The partial pressure of the radiating gas p_p was determined from the following equation obtained from reference 14.

$$p_p = P_g \left(\frac{2.1\, f}{1 + 1.05\, f} \right) \tag{7}$$

It was assumed that for maximum afterburning, the afterburner liner wall would be at a temperature of 923 K (1200° F) at the cruciform beam and then increase linearly in the direction of gas flow to a temperature of 1200 K (1700° F) at the end of the support and then remain constant. The emissivities of the liner wall and support tube walls ϵ_w were assumed to be 0.8.

The convective heat flux into the fuel for each incremental length of cooling tube was obtained from the relation

$$q_F = h_F(T_{wF} - T_F) \tag{8}$$

where the heat-transfer coefficient for the liquid fuel flowing in the tubes was obtained from the correlation equation:

$$\frac{h_{Fd}}{K_F} = 0.005\, Re_F^{0.95}\, Pr_F^{0.4} \tag{9}$$

obtained from reference 15 with a kerosene-type fuel.

The supply pressure of the fuel was assumed to be 413 N/cm^2 (600 psia), which is sufficiently above the critical pressure (182 N/cm^2 (265 psia)) so that the pressure drop in the cooling tubes was not expected to reduce the pressure below critical. As a consequence, the fuel remains a liquid until it is heated above the critical temperature of 653 K (716° F). Above this temperature the heat-transfer correlation (ref. 16) was used for gaseous fuel:

$$\frac{h_{Fd}}{K_F} = 0.023\, Re_F^{0.8}\, Pr_F^{1/3} \left(\frac{\mu_F}{\mu_{Fw}} \right)^{0.14} \tag{10}$$

The effect of tube curvature on the heat-transfer coefficient, was not expected to be large (ref. 15) and was neglected in the present analysis. The fuel Reynolds number and Prandtl numbers and the thermal conductivity in equations (9) and (10) were evaluated at fuel bulk temperature conditions. The fuel viscosities in the numerator and denominator of equation (10) were evaluated at fuel bulk temperature and inside tube wall temperature, respectively. The fuel property values (liquid and gaseous state) were obtained from the Shell Development Company (NASA Contract NAS3-12432) and are shown in table I.

TABLE I. - JET-FUEL PROPERTIES

(a) Liquid

Fuel temperature		Specific heat		Viscosity		Thermal conductivity		Prandtl number	Density	
K	^{o}F	J/(g)(K)	Btu/(lbm)(^{o}F)	N-sec/m^2	lbm/sec-ft	J/(sec)(m)(K)	Btu/(hr)(ft)(^{o}F)		kg/m^3	lbm/ft^3
311	100	2.135	0.510	131.0	88.0	0.156	0.0905	16.90	25.4	1.58
366	200	2.420	.578	58.6	39.4	.140	.0810	10.15	23.9	1.49
422	300	2.680	.640	37.6	25.3	.126	.0730	7.75	22.4	1.40
477	400	2.994	.715	26.5	17.8	.114	.0658	7.10	21.0	1.31
533	500	3.379	.807	16.7	11.2	.102	.0588	5.55	19.2	1.20
589	600	3.936	.940	8.9	6.0	.090	.0520	3.90	16.9	1.06
644	700	6.699	1.60	4.5	3.0	.096	.0555	3.20	11.9	.75

(b) Gas (405 N/cm^2 or 40 atm)

Thermal conductivity, J/(sec)(m) (Btu/(hr)(ft)(^{o}F))	0.059 (0.034)
Gas constant, m/K (ft/^{o}R)	1.54 (9.09)
Specific heat, J/(g)(K) (Btu/(lbm)(^{o}F))	3.85 (0.92)
Viscosity	(a)

[a] $2.62\times10^{-10}\ T^2 - 1.324\times10^{-6}\ T + 1.688\times10^{-3}$ N-sec/m^2 or $5.714\times10^{-10}\ T^2 - 1.602\times10^{-6}\ T + 1.134\times10^{-3}$ lbm/(sec)(ft).

For the analysis conducted herein, the entrance effects were neglected and fully developed turbulent flow conditions were assumed throughout the cooling tubes. The entrance to the cooling tubes is located at the rear of the plug. Here, heat transfer from the gas to the fuel begins. The temperature of the inside tube wall T_{wF} was found by averaging the peripheral temperatures for each incremental cooling tube length. The fuel temperature T_F is the bulk temperature for the incremental length of cooling tube.

The temperature rise in the fuel ΔT_F for each incremental length of cooling tube was obtained from the heat balance:

$$A_O(q_g + q_{rf} + q_{rw}) = A_F q_F = w_F Cp_F \Delta T_F \tag{11}$$

Average fuel and local metal temperatures were determined for each of the 10 incremental lengths of cooling tubes in both the plug and the support tube. The local metal temperatures were determined for each of the nodes in the nodal breakdown of the coolant passage cross section shown in figure 5. The three node locations where the temperatures are of the most interest are the surface nodes indicated by the letters A, B, and C in the figure. These nodes represent the points at which the maximum surface temperature in contact with the gas, the maximum surface temperature in contact with the fuel, and the lowest cross section metal temperature would exist.

Pressure Drop

The pressure drop in the fuel was determined between a point in the toroidal fuel distribution manifold at the rear of the plug and a point after the fuel has cooled the plug and support tube before entering the return manifold. This pressure drop included (1) the entrance loss into the cooling tube from the toroidal supply chamber at the rear of the plug, Δp_e, (2) friction pressure drop Δp_f, and (3) momentum pressure drop Δp_m. These pressure drops were determined by the use of the following equations, adapted from reference 17.

$$\Delta p_e = \frac{1.2\, G^2}{2g\rho_{Fs}} \tag{12}$$

$$\Delta p_f = \sum_{n=1}^{n=20} \frac{4G^2}{gd} \left[\frac{\Delta XF_n}{\left(\frac{\rho_{Fi} + \rho_{Fo}}{2} \right)_n} \right] \tag{13}$$

where

$$F_n = \frac{T_F}{T_{Ff}\left[4.0 \log\left(Re_{Ff} \frac{\rho_{Ff}}{\rho_F} \sqrt{F \frac{T_F}{T_{Ff}}}\right) - 0.4\right]^2} \tag{14}$$

and

$$\Delta p_m = \sum_{n=1}^{20} \frac{G^2}{g}\left(\frac{1}{\rho_{Fo}} - \frac{1}{\rho_{Fi}}\right)_n \tag{15}$$

Structure

Elementary strength of materials theory was used in determining the typical dimensions of the structural elements. Buckling of the plug shell, due to the external gas pressure, is prevented by fastening support rings to the inside surface. The design pressure load supported by the plug shell was assumed to be 34.48 N/cm^2 (50 psia) up to the throat and diminished linearly to zero at the rear of the plug. The spacing of the support rings was determined by using buckling criteria for short cylindrical shells under external pressure where the cylinder diameter is taken to be equal to the large-end diameter of the conical shell. This approach provides a conservative result since the conical shell would be stiffer than the assumed cylindrical shell. The first natural frequency in the lateral mode of vibration of the plug assembly was obtained by assuming the support tube to be a simple cantilever beam extended to the center of gravity of the plug. The mass supported at the end of this beam was taken as the sum of the plug mass and three-eighths of the mass of the support tube assembly. The method used for accounting for the mass of the beam is presented in reference 18. The loads caused by the lateral and longitudinal accelerations due to aircraft motions were applied as statically equivalent loads.

Thermal stresses and strains were calculated by the methods given in reference 19. Temperatures in the shell and tubes were assumed to be constant through the material thickness and equal to the average between the inner and outer surfaces at every location. The shell and tube assembly was uncoupled at the braze joint and the deformations calculated for the shell and tube as separate elements. Since the shell is much stiffer than the tubing, it was conservatively assumed that the deformation of the tubes would be

governed by the shell. The mismatch due to relative deformations between the shell and tube was then used to calculate the resulting strain and stress in the tube.

RESULTS AND DISCUSSION

Temperature Distribution at Shell and Tube Cross Section

The calculated metal temperature distribution for increments of tube length near the nozzle throat is shown in figure 6. Temperatures are shown for conditions of maximum afterburning at sea level with the plug having the cooling tubes with the 0.076-millimeter (0.003-in.) thick walls spaced at two diameters and with full or minimum braze between the plug shell and coolant tubes. The figure shows that the maximum temperature of the plug shell in contact with the gas, as expected, occurred midway between the cooling tubes at node A. The temperature at this location was 807 K (991° F) for the full braze condition and 1049 K (1430° F) for the minimum braze condition. The maximum temperature at the inside wall of the cooling tubes is seen to occur at the centerline of the tube at node B. The temperatures at this location for full and minimum braze conditions were 662 K (732° F) and 820 K (1017° F), respectively. The corresponding fuel temperatures were 519 and 468 K (475° and 383° F), respectively.

Of interest in figure 6 is the rapid reduction in the metal temperature of the inside surface of the cooling tubes at small peripheral distances from the hot spot, and the magnitudes of the metal temperature differences. The first is important, particularly at conditions of minimum braze, because of the reduction of the coking problem at only small distances from the maximum surface-temperature point, and the second is important because of the strains that can be induced by the temperature differences and the possible distortions of the parts that might occur. At a distance of only about one-eighth of a tube circumference from the tube centerline, the surface temperatures dropped from their maximum values by about 17 and 278 K (30 and 500 F$^{\circ}$), for the full and minimum braze conditions, respectively. The extreme in metal temperature differences for the cross sections shown in figure 6 occurs between the extreme in plug shell surface temperature (node A) and the lowest temperature on the inside wall of the cooling tube (node C). The temperature at this node is essentially at the local fuel temperature. As shown in figure 6, the temperature differences between these node locations were 288 K (516 F$^{\circ}$) and 581 K (1047 F$^{\circ}$) for the full and minimum braze conditions, respectively. The temperature differences at these nodes are even larger at the fuel inlet station even though the local metal temperatures are lower. At the fuel inlet this temperature difference was 630 K (1133 F$^{\circ}$) for the minimum braze condition and 361 K (649 F$^{\circ}$) for the full braze condition. The effects of these temperature gradients on thermal stress levels are discussed later.

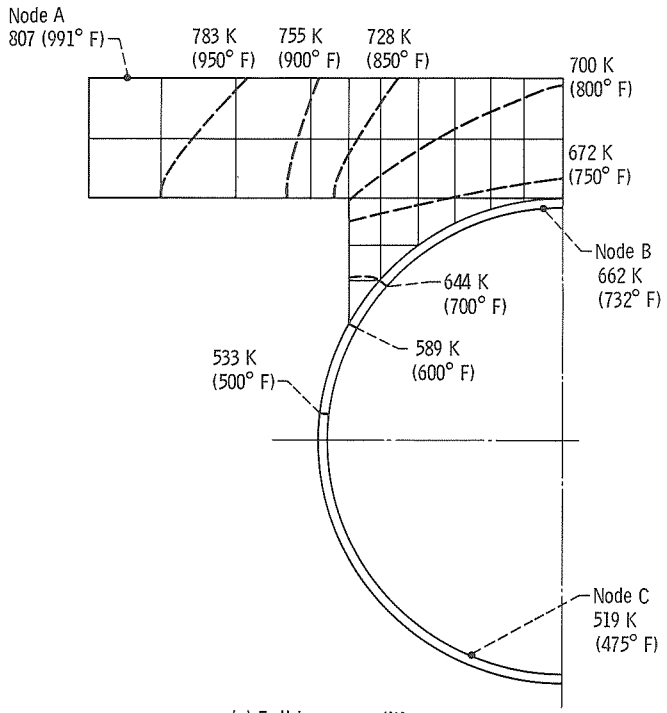

(a) Full braze condition.

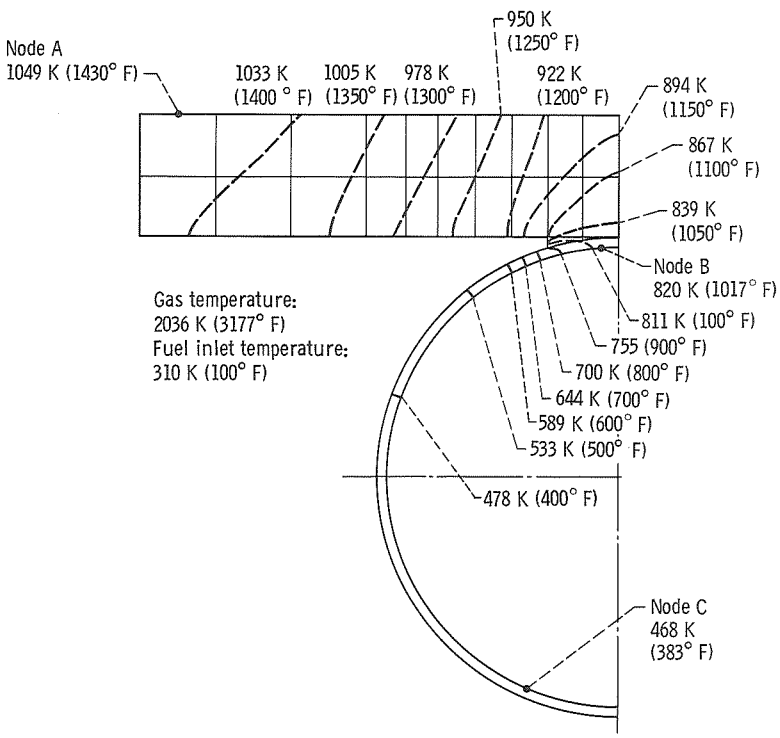

(b) Minimum braze condition.

Figure 6. - Metal temperatures in cooling tubes and shell of plug in region of nozzle throat. Conditions Maximum afterburning at sea level; cooling tubes spaced at 2 diameters; tube wall thickness 0.076 millimeter (0.003 in.).

Temperatures Along Path of Cooling Tubes

The changes in the bulk fuel temperatures and the maximum metal temperatures in the shell gas-side surface and inside surface of the cooling tubes are shown in figures 7 to 12 for various conditions of engine operation, braze amounts between shell and cooling tubes, cooling tube lateral spacings, tube wall thicknesses, fuel inlet temperature, and gas temperature near wall.

Maximum afterburning at sea level. - At this engine condition, the maximum metal temperatures at the outer surface of the shell and inner surface of the cooling tube (nodes A and B, respectively, in fig. 5) generally occurred near the throat of the plug for the tubes spaced at either two or three diameters as shown in figure 7. The effect of tube spacing is seen to be small on comparing the two figures, except for node A. The effect of the amount of braze material is large. For the full braze condition the maximum temperature at node B was about 683 K (770° F) for both the two- and three-tube spacing. At the minimum braze conditions this temperature increased to about 819 K (1015° F) for both tube spacing. These temperatures indicate that even for the minimum braze condition adequate cooling of the metal was attained so that at least 100 hours of operation at this engine condition may be expected without significant coking based on experimental results of low-oxygen-content jet A fuel flowing through heated tubes. Also significant carburization and loss of ductility of tube material is not expected because this problem is not expected to be serious at temperatures below 922 K (1200° F).

Both the tube spacing and the amount of braze material have a large effect on the maximum surface temperature of the plug assembly shell (node A). At the two-diameter tube spacing, figure 7(a) indicates that the maximum temperature at node A was about 805 and 1050 K (990° and 1430° F) for the full and minimum braze conditions, respectively. At the three-diameter tube spacing, figure 7(b) indicates the temperatures at this node location to be 1005 and 1250 K (1350° and 1790° F), respectively. These higher shell metal temperatures and the larger temperature differences between nodes A and B for the three-diameter tube spacing compared with the two-diameter tube spacing favor the selection of the two-tube diameter spacing for cooling the specific plug assembly considered herein. As a consequence, most of the analysis which is reported herein was limited to a plug assembly with cooling tubes spaced at two diameters.

Figure 7 indicates that the fuel remained a liquid in flowing the length of the plug assembly. The fuel exited at a bulk temperature of 602 and 629 K (624° and 673° F) for the minimum and full braze conditions, respectively, for the cooling tubes spaced at two diameters. These temperatures at the three-diameter spacing were 585 and 622 K (594° and 659° F), respectively.

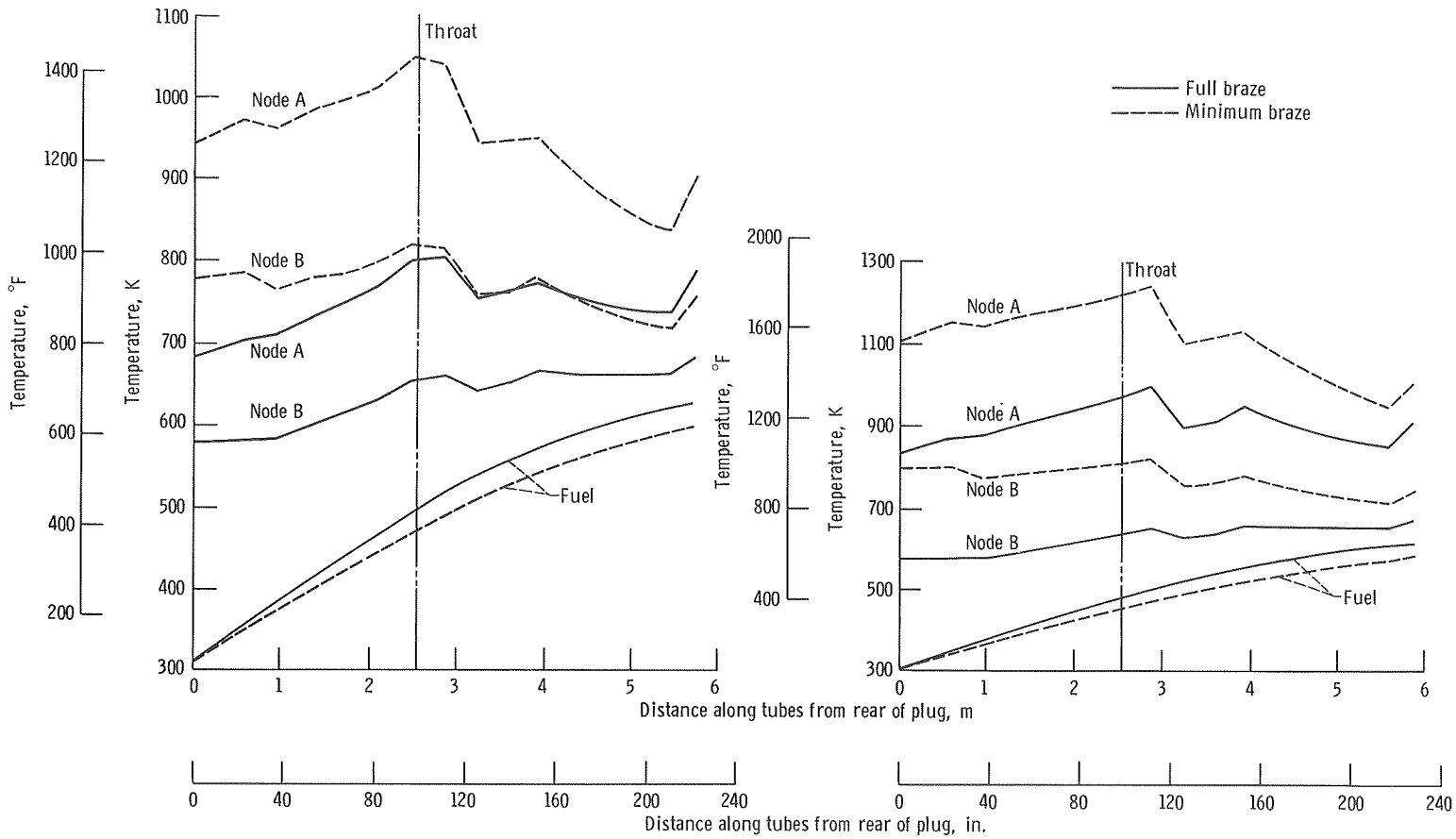

Figure 7. - Temperatures along tubes from rear end of plug to front end of support tube. Conditions: maximum afterburning at sea level; fuel inlet temperature, 311 K (100° F); tube wall thickness, 0.076 millimeter (0.003 in.).

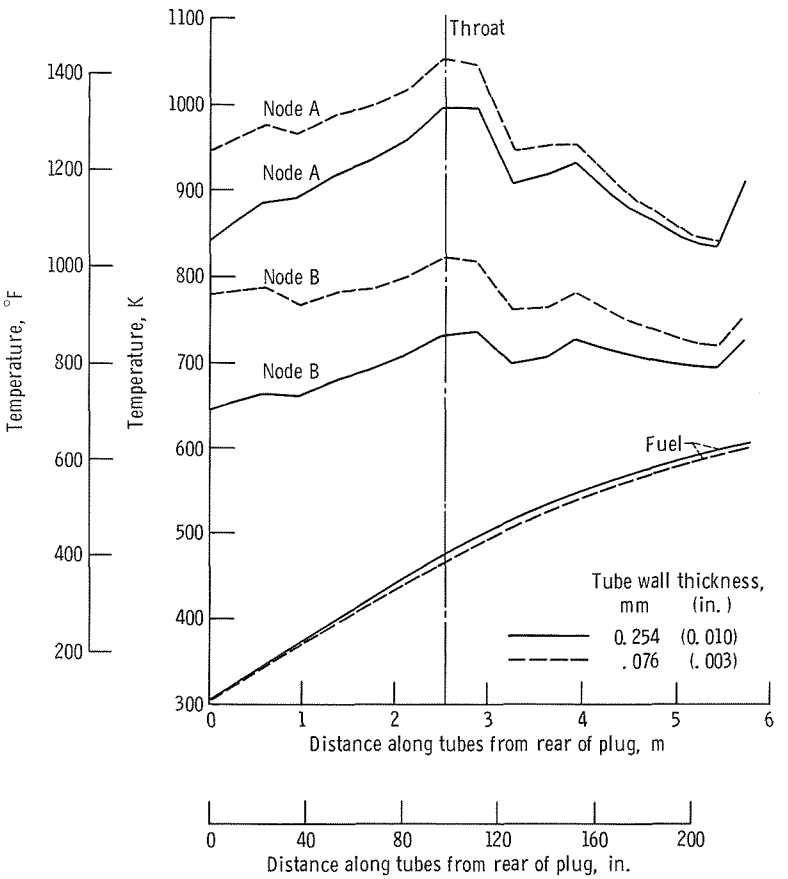

Figure 8. - Effect of tube wall thickness on temperatures along tubes. Conditions: maximum afterburning at sea level; minimum braze between shell and tubes; two-diameter tube spacing.

The effect of increased cooling tube wall thickness on metal and fuel temperatures along the fuel flow path is shown in figure 8. The data are shown for maximum afterburning at sea level and for minimum braze between cooling tubes and shell. Increasing the tube wall thickness from 0.076 to 0.254 millimeter (0.003 to 0.010 in.) reduced the temperatures at nodes A and B by as much as 106 and 133 K (190 and 240 F^{O}). This reduction in temperature occurs at the cooling tube inlet and becomes progressively less along the tube path. At the tube outlet there was essentially no reduction in the temperature at node A and only about 28 K (50 F^{O}) reduction at node B. The increased wall thickness increased bulk fuel temperature by only about 6 K (10 F^{O}). Because the minimum coolant tube wall temperature (node C in fig. 5) is essentially equal to bulk fuel temperature, the maximum temperature difference across the shell and tube cross section (nodes A and C) is reduced from 630 to 535 K (1133^{O} to 960^{O} F) or a reduction in this temperature difference by 95 K (173 F^{O}). Also, this reduction in temperature gradient across the shell and tube further reduces the thermal stresses and leads to a more conservative and somewhat heavier design.

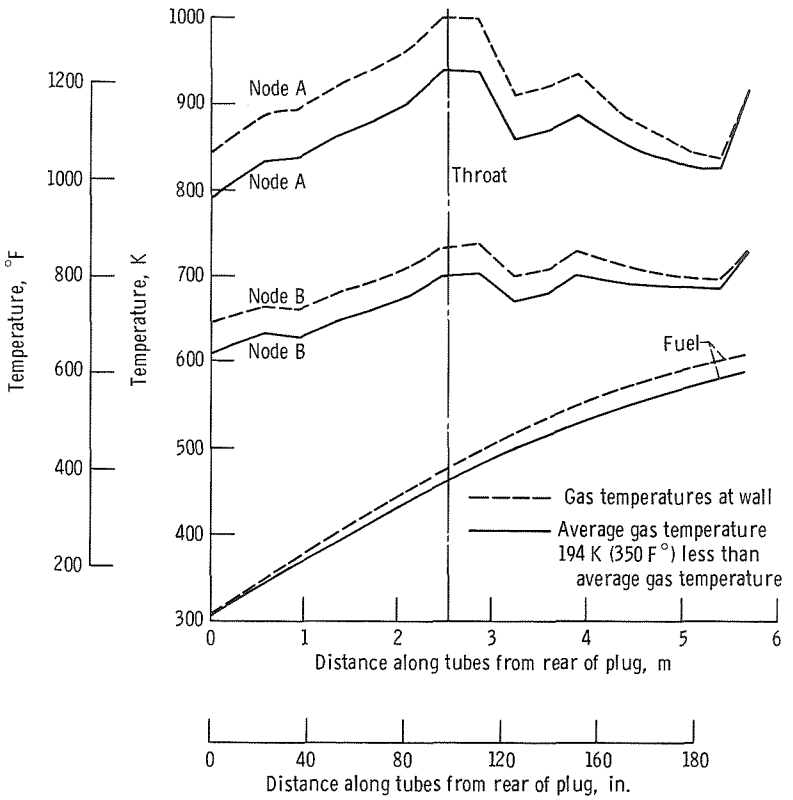

Figure 9. - Effect of gas temperature near wall on temperatures along tubes. Conditions: maximum afterburning at sea level; minimum braze between shell and tubes; tube wall thickness, 0.254 millimeter (0.010 in.).

The predicted metal and fuel temperatures in this report were based on a convective heat flux from the gas using the bulk gas temperature. Because a radial temperature profile will generally exist in the gas passage, the effect of a reduction of 194 K (350° F) in the gas temperature adjacent to the wall (such as obtained in ref. 2) was determined, and the results shown in figure 9. Calculations were made for maximum afterburning at sea level, with two-tube diameter spacing and minimum braze between shell and cooling tubes, and for tube wall thickness of 0.254 millimeter (0.010 in.). The assumed reduction in gas temperature reduced temperatures at node A and B by as much as 56 and 33 K (100 and 60 F°), respectively. The bulk fuel exit temperature decreased by 17 K (30 F°). The maximum metal temperature difference across the shell and tube cross section (nodes A and C, where temperature of node C is essentially equal to bulk fuel temperature) was reduced from 535 to 483 K (960° to 870° F), or a reduction of this temperature difference by 52 K (90 F°).

Maximum afterburning at Mach 1.2 and 13 716 meters (45 000 ft). - Calculated temperatures at nodes A and B at this selected engine condition (fig. 10) were lower than for maximum afterburning at sea level. These results would indicate that the slightly

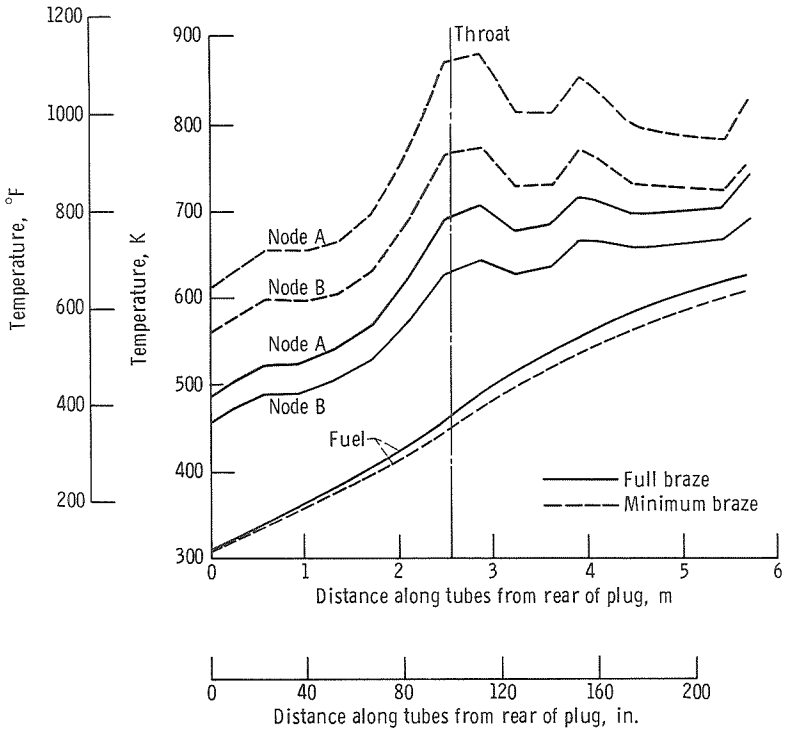

Figure 10. - Temperatures along tubes from rear of plug for maximum afterburning at Mach 1.2 and at an altitude of 13 716 meters (45 000 ft). Fuel inlet temperature, 311 K (100° F); two-diameter-tube spacing; tube wall thickness, 0.076 millimeter (0.003 in.).

lower gas total temperature and lower heat-transfer coefficient combined to more than offset the lower fuel flow rates at the maximum afterburning at the selected flight condition compared with the sea-level condition. The maximum temperatures at the inside of the cooling tubes was about 694 and 778 K (790° and 940° F) for the full and minimum braze condition, respectively. The associated maximum plug outer shell surface temperatures were 744 and 880 K (880° and 1125° F), respectively.

The fuel also remained a liquid in flowing through the plug assembly for these engine conditions. The exit fuel bulk temperatures were 633 and 611 K (670° and 640° F), respectively.

No afterburning at sea level. - For this engine condition all the primary combustor fuel was used to cool the plug. The calculated temperatures at this engine condition are shown in figure 11 for the full and minimum braze conditions for the assumed fuel inlet temperatures of 311 K (100° F). The effect of increasing fuel inlet temperature to 367 K (200° F) is shown in figure 12. As mentioned earlier, the purposes in flowing fuel through the plug assembly at this engine condition are (1) to provide filled cooling tubes and fuel lines to give rapid response of the system for rapid afterburner light-off, (2) to avoid excessive transient thermal stresses in the structure, and (3) to eliminate flow instabilities and coking that may result upon afterburner light-off. Cooling of the plug

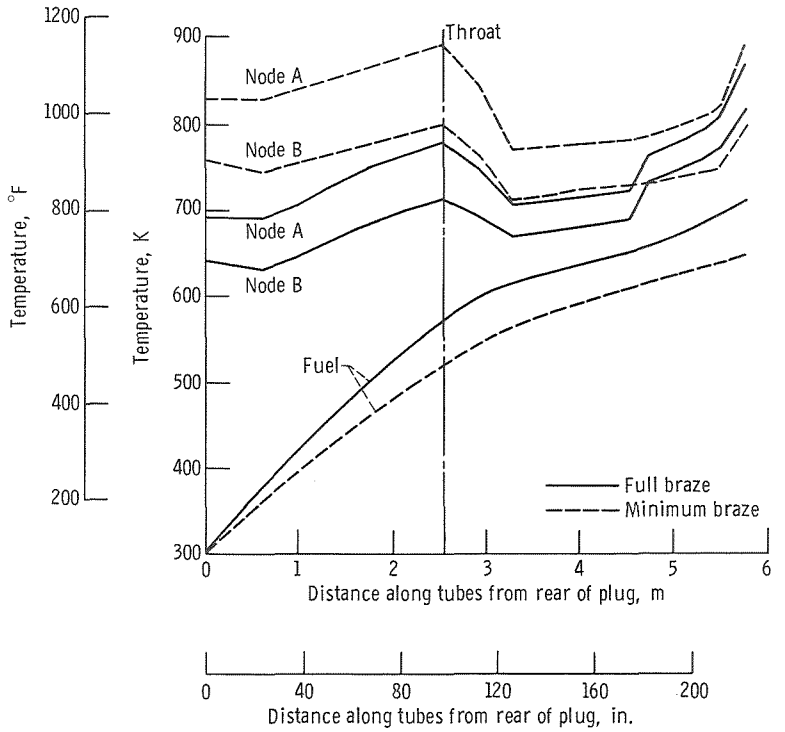

Figure 11. - Temperatures along tubes from rear of plug for conditions of no afterburning at sea level. Fuel inlet temperature, 311 K (100° F); two-diameter-tube spacing; tube wall thickness, 0.076 millimeter (0.003 in.).

shell assembly was not expected to be a problem.

The calculations produced some interesting results. The fuel (fig. 11) leaves the plug assembly as a gas at 652 K (713° F) for the minimum braze tubes and at 714 K (826° F) for the full braze tube even when the fuel inlet temperature was 311 K (100° F). For the full braze condition, the fuel becomes a gas at a point about 4.57 meters (180 in.) from the rear of the plug along the fuel path. At this location the fuel-side heat-transfer coefficient decreases with an attendant rapid rise in the inside tube wall temperature. Figure 11 shows that the maximum inside wall temperature (node B) for the full braze tubes exceeds that of the minimum braze tube in which the fuel only becomes a gas at the exit. Thus despite the lower gas total temperature of 985 K (1310° F) with no afterburning compared with 2036 K (3177° F) with afterburning, the reduced fuel flow in the plug assembly when not afterburning results in higher fuel temperature rises and higher inside wall temperatures than when afterburning. Figure 11 shows that for the 311 K (100° F) fuel inlet temperature the maximum metal temperature for node B was 817 K (1010° F) for the full braze tubes and 800 K (980° F) for the minimum braze tubes. These results indicate that the effect of the amount of braze on the inside wall temperatures at this engine condition is not large. Even at these temperatures, however, coking is not expected to be significant for at least 100 hours of engine operation.

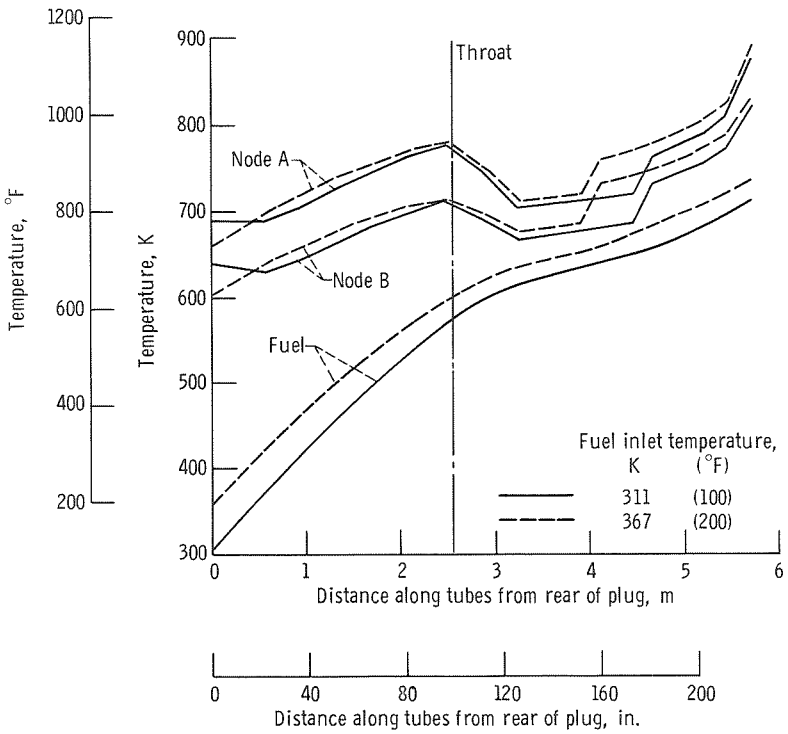

Figure 12. - Effect of fuel inlet temperature on temperatures along tubes. Conditions: no afterburning at sea level; full braze between shell and tubes; two diameter tube spacing; tube wall thickness, 0.076 millimeter (0.003 in.).

Temperatures are lower away from this point along the fuel flow path or around the periphery of the cooling tube. As an example, at a peripheral distance of less than one-fourth of the tube circumference the surface temperature dropped 76 K (137 F^{O}) below the maximum value.

Because the sea-level, nonafterburning condition is limiting relative to coking deposits, it is fortunate that the period of time spent at this engine condition is small. It is also fortunate that increases in inlet fuel temperature do not have a large effect on maximum inside tube wall temperature, which would further aggravate the problem. As shown in figure 12 increasing the fuel inlet temperature from 311 to 367 K (100^{O} to 200^{O} F) for a full braze tube condition resulted in the maximum inside wall temperature increasing by only 10 K (20 F^{O}). When the fuel entered the plug assembly at 367 K (200^{O} F), it exited at a temperature of 738 K (869^{O} F).

The plug assembly shell temperatures, which are not expected to be a problem at the relatively low nonafterburning gas temperature, reached a maximum value (node A in figs. 11 and 12) of about 889 K (1140^{O} F).

The results obtained at sea-level nonafterburning condition indicate that the primary combustor would need to be designed to burn gaseous fuel. When the afterburner is lit, however, the fuel exits from the plug assembly as a liquid. As a consequence, a

scheme is needed that would avoid the complexity of a dual (liquid and gas) injection system for the primary burner and the problems associated with the metering of the fuel in two phases. One possible scheme is to take the portion of the liquid fuel from the plug assembly that is designated for the primary combustor and permit it to dwell within the cruciform support beam so that it would pick up heat and become a gas. Another possible scheme would be to reduce the heat flux into the fuel and keep it a liquid. This, as an example, could be done by use of a ceramic coating or a double outer shell construction.

Fuel Pressure Drop

The calculated fuel pressure drop between the fuel supply toroidal chamber at the rear of the plug and the cooling tube exit was small. The maximum pressure drop occurred for the cooling tubes spaced at three diameters. This higher pressure drop was due primarily to the higher flow rate per tube that resulted when 34 tubes were used for the three-diameter tube spacing instead of the 50 tubes used for the two-diameter tube spacing. At the three-diameter tube spacing with the plug nozzle operating at maximum afterburning at sea level, the fuel pressure drop was 54 N/cm^2 (79 psi). The effect of full or minimum braze on the pressure drop was small since the pressure drop was primarily due to friction. For the two-diameter tube spacing at this nozzle condition the fuel pressure drop was 26 N/cm^2 (38 psi). The fuel pressure drops with maximum afterburning at Mach 1.2 at an altitude of 13 716 meters (45 000 ft) and for nonafterburning at sea level were approximately the same at 4.8 N/cm^2 (7 psi) with the cooling tube spaced at two diameters.

Structures

The stress analysis made in support of the design showed that, at a design peak fuel pressure of 621 N/cm^2 (900 psia), the hoop stress in the coolant tube wall would be 13 450 N/cm^2 (19 500 psi). The maximum bending stress in the support tube, for a lateral acceleration of four times the acceleration of gravity was 10 620 N/cm^2 (15 400 psi). The stiffening ring for the frontal cone on the plug was located so as to give a 50-percent margin of safety on the design pressure of 34.5 N/cm^2 (50 psia). The first natural frequency of the plug-support-tube assembly, in the lateral mode of vibration, was determined to be 15 hertz.

The stress levels due to pressure and acceleration loadings are low enough so that the selection of materials of construction, from available high-temperature alloys, provides some flexibility. A material with an elongation property of 20 percent or better

should provide adequate capability to accommodate localized yield stresses at discontinuities, should they exist.

Temperature distributions as shown in figure 6, for throat region, are quite representative and indicate a potential thermal stress problem. Conditions at the rear end of the plug are more severe than those at the throat. For maximum afterburning at sea level the temperature gradients associated with the minimum braze case (most severe condition) can produce yielding in the tube wall at the braze joint. Plastic deformation in tension of the tubing at the joint was calculated to be about 0.8 percent for the minimum braze case. Further, for engine shutdown and return of tubing to ambient temperatures, compressive yielding of about 0.3 percent in the tubing is predicted. This indicates potential failure by a ratcheting mechanism. At the rear of the plug for the full braze case, a permanent set of 0.13 percent was calculated for the tube with no yielding on cooling to ambient temperature. This indicates no problem with a life limiting situation as for the minimum braze case. For all conditions considered in this work no plastic deformation of the plug shell was revealed by the analysis.

The foregoing results were for a cooling tube thickness of 0.076 millimeter (0.003 in.). This thickness selection was governed by that required to sustain the fuel pressure and minimize weight. Special handling precautions must be observed in working with this size of tubing to prevent damaging it.

The effect of increasing tube wall thickness to 0.254 millimeter (0.010 in.) results in reductions of the maximum metal temperature differences. These reductions in metal temperature differences should result in lower thermal stresses than for the thinner wall tubing.

Weights

The total dry weight of the plug, supporting structure, and manifold assemblies with 0.076-millimeter (0.003-in.) thick cooling tubes was 27 kilograms (60 lbm). If cooling tubes with 0.254-millimeter (0.010-in.) wall thickness are used, the dry weight increases 7 percent. The wet weight of the assembly with thin tubes is 35 kilograms (77 lbm). These weights were determined from the layout drawings from which figure 3 was derived.

OTHER CONSIDERATIONS

Even though temperatures of the wall in contact with the fuel were low enough to expect at least 100 hours of engine operation without significant coking in the nozzle, coke buildup with time may eventually become unacceptable. At that time a scheme for

the removal of the accumulated deposits by burning could be used. This could be done, as suggested in reference 6, by passing 922 K (1200° F) air through the tubes while the engine is not operating.

Even though the analysis indicated that the fuel-cooled plug is structurally feasible for the full braze condition, it will be necessary, for a specific detailed design, to investigate several problem areas. Some of these are the thermal stresses between tubes and shell, the vibrations due to gas flow disturbances and resonances in the structure, potential pressure pulsations in the coolant tubes due to sudden changes in heat-transfer characteristics in the tubes, and the effect of tolerances on minimum thicknesses for structure components.

The brazing method of joining the coolant tubes to the shell is practical and reliable if specific procedures are followed (discussed in ref. 20). Strengths of brazed joints are dependent on many factors such as joint clearance, joint geometry, base metal alloy, and filler metal composition. Working stresses were not assigned to the brazed joints because these factors were too complex. The most reliable way to insure successful braze joints is to subject full scale specimens to tests representing service conditions.

SUMMARY OF RESULTS

1. A conceptual design of a jet fuel-cooled plug nozzle was evolved which is structurally feasible and can be regeneratively cooled with the available primary and afterburner fuel flow.

2. Coking of the fuel passages would be most likely when operating at nonafterburning, sea-level takeoff conditions. Despite the lower gas total temperature when not afterburning, the associated lower fuel flow available for cooling the plug assembly resulted in both higher fuel temperatures and higher coolant-tube inside-wall metal temperatures. The maximum inside tube-wall temperature was 817 K (1010° F).

3. At sea-level maximum afterburning, the maximum inside tube-wall temperature was about 683 K (770° F).

4. No significant coke deposits on the tube walls should be expected at these wall temperatures for periods of at least 100 hours based on experiments with fuel flowing through heated tubes. Coking at other than the maximum temperature point on the tube locations should be considerably less. For example, at a peripheral distance of slightly less than one-fourth of the tube inside-circumference from the maximum temperature point, a drop in temperature of about 76 K (137 F°) would occur for the condition of no afterburning at sea level.

5. The spacing of the cooling tubes has a small effect on the tube inside surface temperatures but has a large effect on the plug-assembly shell outer surface temperature, particularly if a minimum braze condition exists. The maximum shell outer sur-

face temperature was 1050 K (1430° F) for a two-diameter tube spacing and 1250 K (1790° F) for a three-diameter tube spacing. The three-diameter tube spacing also increased temperature differences in the structure, thus increasing thermal stresses and distortions. These factors would favor the selection of a two- rather than a three-diameter tube spacing.

6. The amount of braze between cooling tube and plug shell affected both inside tube-wall and outer-shell temperatures. The maximum inside tube-wall surface temperature was generally about 56 to 222 K (100° to 400° F) higher for the minimum than for the full braze. The maximum temperature point on the outer shell of the plug was also higher by about 22 to 278 K (40 to 500 F°).

7. Increasing the cooling-tube wall thickness and decreasing the gas temperature near the wall to account for radial profile in the gas temperature reduces the metal temperature differences between the plug shell and cooling tubes and the inside tube wall temperatures. These lower temperatures would reduce thermal stresses and coking. Increasing the tube wall thickness from 0.076 to 0.254 millimeter (0.003 to 0.010 in.) for minimum braze condition reduced the maximum metal temperature difference in the plug shell and cooling tube cross section by 95 K (173 F°) and the maximum inside tube wall temperature by 133 K (240 F°). Decreasing the gas temperature near the plug shell by 194 K (350° F) at this increased tube wall thickness further reduced these temperatures by 52 K (90 F°) and 33 K (60 F°), respectively.

8. Stresses due to pressure and acceleration loadings were calculated to be less than 20 percent of the yield strength.

9. Thermal stresses were calculated to be above yield in the tubing at the rear end of the plug for the thin wall design for the most severe temperature conditions. For the maximum braze case the plastic deformation was calculated to be 0.13 percent with no yielding on engine shutdown. Therefore, a ratcheting type failure is not anticipated for the full braze case.

10. For all the conditions considered no plastic deformation of the plug shell was predicted.

Lewis Research Center,
National Aeronautics and Space Administration,
Cleveland, Ohio, March 26, 1971,
720-03.

APPENDIX - SYMBOLS

A_F fuel tube surface area for increment of cooling tube length

A_O outside shell surface area for increment of cooling tube length

Cp_F specific heat of fuel at constant pressure

d cooling tube inside diameter

F Fanning friction factor

f local fuel-air ratio

G fuel flow per unit area

g gravitational constant

h_F fuel-side heat-transfer coefficient

h_g gas-side heat-transfer coefficient

K_F fuel thermal conductivity

l mean beam path length $= \left(\frac{3.6 \text{ volume}}{\text{surface area}}\right)$

M_g gas Mach number

P_g gas total pressure

Pr_F fuel Prandtl number

Pr_g gas Prandtl number

p_g gas static pressure

p_p partial pressure of radiating gas

Δp_e pressure drop at entrance to fuel tube

Δp_f pressure drop in fuel due to friction

Δp_m pressure drop in fuel due to momentum change

q_F convective heat flux into fuel per unit area

q_g convective heat flux from gas per unit area

q_{rf} radiation heat flux from flame per unit area

q_{rw} radiation heat flux interchange between walls or boundaries per unit area

Re_F fuel Reynolds number based on bulk temperature

Re_{Ff} fuel Reynolds number based on film temperature

r_s outside radius of support tube

r_t	inside radius of tailpipe
T_F	fuel bulk temperature
T_{Ff}	fuel film temperature
T_f	flame temperature
T_g	total gas temperature
T_{ge}	effective gas temperature
T_{wF}	inside-wall temperature of cooling tubes
T_{wo}	shell outside surface temperature
T_{ws}	outside-wall temperature of support tube
T_{wt}	inside-wall temperature of tailpipe
ΔT_F	temperature rise of fuel
w_F	fuel flow rate per tube
X_s	distance from reference point to incremental length of support tube
X_t	distance from reference point to incremental length of tailpipe
ΔX	incremental length of cooling tube
α_w	wall absorbtivity
Γ	transmittance of gas (eq. (6))
γ	ratio of specific heats of the gas
δ	incremental axial length, support tube and tailpipe
ϵ_f	emissivity of flame
ϵ_w	emissivity of walls
Λ	recovery factor
μ_F	fuel viscosity based on bulk temperature
μ_{FW}	fuel viscosity based on wall temperature
ρ_F	average fuel density for increment of tube length, based on bulk temperature
ρ_{Ff}	average fuel density for increment of tube length, based on film temperature
ρ_{Fi}	fuel density at inlet to incremental length of cooling tube
ρ_{Fo}	fuel density at outlet from incremental length of cooling tube
ρ_{Fs}	fuel density at cooling tube inlet

σ Stefan-Boltzmann constant

Subscript:

n index of summation, identifies increment of cooling tube length

REFERENCES

1. Bresnahan, Donald L.: Experimental Investigation of a 10° Conical Turbojet Plug Nozzle with Iris Primary and Translating Shroud at Mach Numbers from 0 to 2.0. NASA TM X-1709, 1968.

2. Clark, John S.; Graber, Edwin J.; and Straight, David M.: Experimental Heat Transfer and Flow Results from an Air-Cooled Plug Nozzle System. NASA TM X-52897, 1970.

3. Chenoweth, Francis C.; and Lieberman, Arthur: Experimental Investigation of the Heat Transfer Characteristics of a Film-Cooled Plug Nozzle with a Translating Shroud. NASA TN D-6160, 1971.

4. Anon.: Hydrocarbon SCRAMJET Feasibility Program. Vol. 1. Engine and Cooling Investigations. Rep. 6129, vol. 1, Marquardt Corp. (AFAPL-TR-67-97, vol. 1, DDC No. AD-384567L), Sept. 1967.

5. Hines, W. S.; and Wolf, H.: Pressure Oscillations Associated with Heat Transfer to Hydrocarbon Fluids at Supercritical Pressures and Temperatures. ARS J., vol. 32, no. 3, Mar. 1962, pp. 361-366.

6. Watt, James J.; Evans, Albert, Jr.; and Hibbard, Robert R.: Fouling Characteristics of ASTM Jet A Fuel When Heated to 700° F in a Simulated Heat Exchanger Tube. NASA TN D-4958, 1968.

7. Nixon, A. C.; Ackerman, G. H.; Hawthorn, R. D.; Henderson, H. T.; and Ritchie, A. W.: Vaporizing and Endothermic Fuels for Advanced Engine Application. Rep. S-14007, Shell Development Co., Aug. 1966. (Available from DDS as AD-801028.)

8. Huntley, Sidney C.; and Samanich, Nick E.: Performance of a 10° Conical Plug Nozzle Using a Turbojet Gas Generator. NASA TM X-52570, 1969.

9. Anon.: Model Specification E1075; Engine, Aircraft, Turbojet, J85-GE-13. General Electric Co., June 1963.

10. Chambellan, Rene E.; and Pleban, Eugene J.: Involute Strip Development Method for Fabrication of Rotationally Symmetrical Double Curved Surfaces of Revolution. NASA TN D-6050, 1970.

11. Lewis, D. R.; Gaski, J. D.; and Thompson, L. R.: Chrysler Improved Numerical Differencing Analyzer for 3rd Generation Computers. Rep. TN-AP-67-287, Chrysler Corp. (NASA CR-99595), Oct. 20, 1967.

12. Elliott, David G.; Bartz, Donald R.; and Silver, Sidney: Calculation of Turbulent Boundary-Layer Growth and Heat Transfer in Axisymmetric Nozzles. Tech. Rep. 32-387, Jet Propulsion Lab., California Inst. Tech., Feb. 15, 1963.

13. Anon.: Computer Program for the Analysis of Annular Combustors. Vol. I: Calculation Procedures. Rep. 1111-1, vol. 1, Northern Research and Engineering Corp. (NASA CR-72374), Jan. 29, 1968.

14. Lefebvre, A. H.; and Herbert, M. V.: Heat-Transfer Processes in Gas-Turbine Combustion Chambers. Proc. Inst. Mech. Eng., vol. 174, no. 12, 1960, pp. 463-478.

15. Hines, W. S.: Investigation of Cooling Problems at High Chamber Pressures. Rep. 3999, Rocketdyne Div., North American Aviation. (NASA CR-50773), May 1963.

16. Knudsen, James G.; and Katz, Donald L.: Fluid Dynamics and Heat Transfer. McGraw-Hill Book Co., Inc., 1958.

17. Chenoweth, Francis C.; Watt, James J.; and Sprague, Earl L.: Transient Chilldown of a Single Thick-Walled Tube by Liquid and Gaseous Hydrogen. NASA TN D-4238, 1967.

18. Freberg, Carol R.; and Kemler, E. N.: Elements of Mechanical Vibration. Second ed., John Wiley & Sons, Inc., 1949, pp. 143-147.

19. Timoshenko, S.; and Goodier, J. N.: Theory of Elasticity. Second ed., McGraw-Hill Book Co., Inc., 1951, pp. 399-404.

20. American Welding Society: Brazing Manual, Second ed., Reinhold Publ. Corp., 1963.

NASA-Langley, 1971 — 28 E-6022

NATIONAL AERONAUTICS AND SPACE ADMINISTRATION
WASHINGTON, D. C. 20546

OFFICIAL BUSINESS
PENALTY FOR PRIVATE USE $300

FIRST CLASS MAIL

POSTAGE AND FEES PAID
NATIONAL AERONAUTICS AND
SPACE ADMINISTRATION

POSTMASTER: If Undeliverable (Section 158 Postal Manual) Do Not Return

"The aeronautical and space activities of the United States shall be conducted so as to contribute . . . to the expansion of human knowledge of phenomena in the atmosphere and space. The Administration shall provide for the widest practicable and appropriate dissemination of information concerning its activities and the results thereof."

—NATIONAL AERONAUTICS AND SPACE ACT OF 1958

NASA SCIENTIFIC AND TECHNICAL PUBLICATIONS

TECHNICAL REPORTS: Scientific and technical information considered important, complete, and a lasting contribution to existing knowledge.

TECHNICAL NOTES: Information less broad in scope but nevertheless of importance as a contribution to existing knowledge.

TECHNICAL MEMORANDUMS: Information receiving limited distribution because of preliminary data, security classification, or other reasons.

CONTRACTOR REPORTS: Scientific and technical information generated under a NASA contract or grant and considered an important contribution to existing knowledge.

TECHNICAL TRANSLATIONS: Information published in a foreign language considered to merit NASA distribution in English.

SPECIAL PUBLICATIONS: Information derived from or of value to NASA activities. Publications include conference proceedings, monographs, data compilations, handbooks, sourcebooks, and special bibliographies.

TECHNOLOGY UTILIZATION PUBLICATIONS: Information on technology used by NASA that may be of particular interest in commercial and other non-aerospace applications. Publications include Tech Briefs, Technology Utilization Reports and Technology Surveys.

Details on the availability of these publications may be obtained from:

SCIENTIFIC AND TECHNICAL INFORMATION OFFICE

NATIONAL AERONAUTICS AND SPACE ADMINISTRATION

Washington, D.C. 20546